

Towards Partner-Aware Humanoid Robot Control under Physical Interactions

Yeshasvi Tirupachuri¹, Gabriele Nava², Diego Ferigo², Luca Tagliapietra², Claudia Latella², Daniele Pucci²

Abstract—The topic of physical human-robot interaction received a lot of attention from the robotics community because of many promising application domains. However, studying physical interaction with a robot by an external agent, like a human or another robot, without considering the dynamics of both the systems involved leads to many short comings in fully understanding and exploiting the interaction. In this paper we present a coupled-dynamics formalism followed by a sound approach in exploiting helpful interaction with a humanoid robot. Furthermore, we present a task-based partner-aware robot control techniques. The theoretical results are validated by conducting experiments with two iCub humanoid robots involved in a physical interaction.

Index Terms—physical Robot-Robot Interaction, physical Human-Robot Interaction, Humanoids.

I. INTRODUCTION

The evolution of robotic systems over the last decade is much more rapid than it has ever been since their debut. Robots existed as separate entities till now but the horizons of a symbiotic human-robot partnership is impending. In particular, application domains like elderly care, collaborative manufacturing, collaborative manipulation, etc., are considered the need of the hour. Across all these domains, it is crucial for robots to physically interact with humans to either assist them or to augment their capabilities. Such *human in the loop* physical human-robot interaction (pHRI) scenarios demand careful consideration of both the human and the robot systems while designing controllers to facilitate robust interaction strategies for successful task completion. More importantly, a generalized human-robot interaction formalism is needed to study the physical interaction adaptation and exploitation. Towards that goal, in this paper we present a generalized human-robot interaction formalism and partner-aware robot control techniques.

The three main components of any pHRI scenario are: 1) a *robotic agent*, 2) a *human agent* and, 3) the *environment* surrounding them. Over the course of time, physical interactions are present between any of the two components. An intuitive conceptual representation of the interactions occurring during pHRI is presented in [1]. More specifically, interaction between a human and a humanoid robot is particularly challenging because of the complexity of the

*This work is supported by PACE project, Marie Skłodowska-Curie grant agreement No 642961 and An.Dy project which has received funding from the European Union's Horizon 2020 Research and Innovation Programme under Grant Agreement No. 731540.

¹Department of Robotics, Brains and Cognitive Sciences, Istituto Italiano di Tecnologia, Genova, Italy name.surname@iit.it

²Department iCub Facility, Istituto Italiano di Tecnologia, Genova, Italy name.surname@iit.it

robotic system [2]. Unlike traditional industrial robots which are fixed base by design, humanoid robots are designed as floating base systems to facilitate anthropomorphic navigational capabilities. The aspect of balancing has received a lot of attention in the humanoid robotics community and several prior efforts [3] [4] [5] went in to building controllers that ensure stable robot behavior. More recently momentum-based control proved to be a robust approach and several successful applications have been realized [6] [7] [8] [9] ensuring contact stability [10] with the environment by monitoring contact wrenches through quadratic programming [11] [12] [13]. In general, these controllers are built to be robust to any external perturbations and hence they are often blind to any helpful interaction a human is trying to have with the robot to help achieve its task.

The knowledge of human intent is a key element for successful realization of pHRI. The process of human intent detection is broadly divided into *intent information*, *intent measurement* and *intent interpretation* [1]. The choice of a communication channel is directly related to intent measurement and affects the robot's ability to understand human intent. Accordingly, a myriad of technologies have been used as interfaces for different applications of pHRI. In the context of rehabilitation robotics, electroencephalography (EEG) [14] [15] [16] and electromyography (EMG) [17] [18] [19] [20] proved to be invaluable. Force myography (FMG) [21] [22] [23] is a relatively new technology which has been successfully used in rehabilitation. EMG has also been successfully used by [24] to realize a pHRI collaborative application to continuously monitor human fatigue. Force/Torque sensors mounted on the robots are often the most relied technology in pHRI scenarios for robot control as they facilitate direct monitoring and regulation of the interaction wrenches between the human and the robot [25] [26] [27] [28] [29]. Vision based techniques like human skeletal tracking [30], human motion estimation [31] and hand gesture recognition [32] are also used as interfaces.

In general, the designer decides on the choice of the interface depending on the application and often using a single mode of interface is limiting. Hence, a combination of vision and haptic interfaces are used in literature to realize successful applications of human robot collaboration [33] [34]. However, we believe there is an impending change in this paradigm and the future technologies of pHRI will leverage on getting as much holistic information as possible from humans involved in pHRI, especially for domains like collaborative manufacturing. Having both the kinematic quantities like joint positions and velocities and dynamic

quantities like joint accelerations and torques of the human will enable real-time monitoring of the human dynamics to build robust controllers for successful task completion taking into account the physical interactions between the human and the robot.

In a typical physical interaction scenario, the dynamics of the two agents involved play a crucial role in shaping the interaction. So, in order to understand the interaction more concretely the dynamics of both the systems has to be considered together rather than in isolation. In this paper we take into account the dynamics of the combined system and present a *coupled-dynamics formalism* followed by a sound approach in exploiting helpful interaction with the robot. Furthermore, we present a task-based partner-aware robot control techniques. We validate our approach using an experimental scenario in which assistance provided by an external interacting agent is leveraged by the robot for its task completion. This paper is organized as follows: Section II introduces the notations, the system modeling and the typical contact constraints. Section III presents the task-based control law. Section IV lays the details of the experiments conducted. Section V presents the results followed by conclusions and further extensions.

II. BACKGROUND

A. Notation

In this section we present the basic notation used in this paper. A denotes an inertial frame, with z -axis pointing against the gravity. The constant g denotes the norm of the gravitational acceleration. We advise the reader to pay close attention to the notational nuances. The human-related notations are denoted with double – bold terms, e.g., \mathbf{n} , robot-related notations are denoted with “straight” terms, e.g., n , and notations that apply to both the systems are denoted with *slanted* terms, e.g., \mathbf{n} . In addition, composite matrices are denoted with ***BOLD*** terms, e.g., \mathbf{M} .

B. Modeling

A typical physical human-robot interaction scenario is shown in Fig. 1. There are two agents: the human, and the robot. Both agents are physically interacting with the environment and, in addition, are also engaged in physical interaction with each other.

In the first approximation, both the human and the robot can be considered as multi-body mechanical systems composed of $n + 1$ and $n + 1$ rigid bodies respectively, called links, connected through $m \in \mathbb{N}$ and $n \in \mathbb{N}$ joints with one degree of freedom. Even though the assumption of human body being modeled as rigid bodies is far from reality, it serves as a rough approximation when formulating physical human-robot interaction dynamics and allow us to synthesize robot controllers optimizing both human and robot variables. Further, we consider both the human and the robot to be *free-floating* systems, i.e. none of the links have an *a priori* constant pose with respect to the inertial frame.

The configuration space of a *free-floating* system is characterized by the *joint positions* and the pose of a specific

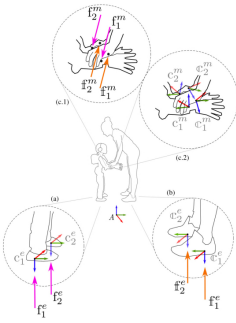


Fig. 1: A typical human-robot dynamic interaction scenario

frame attached to a link of the system, generally referred to as *base frame* denoted by B . In the case of a *free-floating* mechanical system, the configuration space is a set of elements representing the *floating base* and the total number of joints, say n . Hence, it lies on the Lie group $\mathbb{Q} = \mathbb{R}^3 \times SO(3) \times \mathbb{R}^n$. We denote an element in the configuration space with $q = (q_b, s) \in \mathbb{Q}$. It consists of pose of the *base frame* $q_b = (^A p_B, ^A R_B) \in \mathbb{R}^3 \times SO(3)$ where $^A p_B \in \mathbb{R}^3$ denotes the position of the base frame with respect to the inertial frame; $^A R_B \in SO(3)$ denotes the rotation matrix representing the orientation of the base frame with respect to the inertial frame; and the joint positions vector $s \in \mathbb{R}^n$ capturing the topology (*shape*) of the robot. Specifically, $\mathbf{q} \in \mathbb{Q}$ denotes an element of the human configuration space and $\mathbf{q} \in \mathbb{Q}$ denotes an element of the robot configuration space.

To the purpose of finding mathematical models for both the (approximation of the) human and the robot, we apply the Euler-Poincaré formalism to both multi-body systems [35]. Then, we obtain the following equations of motion describing the dynamics of the human and the robotic agents respectively:

$$\mathbb{M}(\mathbf{q})\dot{\mathbf{v}} + \mathbb{C}(\mathbf{q}, \mathbf{v})\mathbf{v} + \mathbb{G}(\mathbf{q}) = \mathbb{B}\tau^H + \mathbb{J}^T \mathbb{f}^* \quad (1a)$$

$$M(q)\dot{\nu} + C(q, \nu)\nu + G(q) = B\tau^R + J^T f^* \quad (1b)$$

In general, $M \in \mathbb{R}^{n+6 \times n+6}$ is the mass matrix, $C \in \mathbb{R}^{n+6 \times n+6}$ is the Coriolis matrix, $G \in \mathbb{R}^{n+6}$ is the gravity term, $B = (0_{n \times 6}, 1_n)^T$ is a selector matrix, $\tau^{\text{H,R}} \in \mathbb{R}^n$ is a vector representing the agent joint torques. Here, n is the number of joints that are assumed to compose either the model of the human or that of the robot, and may be different in the two cases. We also assume that each agent, is subject to a total of $n_c = n_m + n_e \in \mathbb{N}$ distinct wrenches. These wrenches are composed of two subsets: the wrenches due to *mutual* interaction, denoted with the subscript m and the wrenches exchanged between the *agent* and the *environment*, denoted with the subscript e respectively. In either case, the contact wrenches are represented by:

$$f^* = \begin{bmatrix} f_1^m; & f_2^m; & \dots & f_{n_m}^m; \\ f_{n_e+1}^e; & f_{n_e+2}^e; & \dots & f_{n_e}^e \end{bmatrix} \in \mathbb{R}^{6n_c}$$

Accordingly, $\mathbb{F}^* = [\mathbb{f}_m \quad \mathbb{f}_e]^T$ with \mathbb{f}_m the external wrenches applied on the human agent by the robotic agent and \mathbb{f}_e the external wrenches applied on the human agent by the environment. Similarly, $\mathbf{f}^* = [f_m \quad f_e]^T$ with f_m the external wrenches applied on the robotic agent by the human agent and f_e the external wrenches applied on the robotic agent by the environment.

We define a set of frames $\mathcal{C} = \{c_1, c_2, \dots, c_{n_e}, c_{n_e+1}, c_{n_e+2}, \dots, c_{n_m}\}$ and assume that the application point of the k -th external wrench on an agent is associated with a frame $c_k \in \mathcal{C}$, attached to the agent link on which the wrench acts, and has z -axis pointing in the direction normal to the contact plane. Furthermore, the external wrench f_k^e is expressed in a frame whose orientation is that of the inertial frame A , and whose origin is that of the frame c_k .

The jacobian $J_{c_k} = J_{c_k}(q)$ is the map between the agent's velocity $\nu = [\nu_B; \dot{s}] \in \mathbb{R}^{n+6}$ and the velocity of the frame c_k given by ${}^A v_{c_k} = [{}^A \dot{p}_{c_k}; {}^A \omega_{c_k}]$:

$${}^A v_{c_k} = J_{c_k} \nu \quad (2)$$

The jacobian matrix has the following structure [36]:

$$J_{c_k}(q) = \begin{bmatrix} J_{c_k}^b(q) & J_{c_k}^j(q) \end{bmatrix} \in \mathbb{R}^{6 \times n+6} \quad (3a)$$

$$J_{c_k}^b(q) = \begin{bmatrix} 1_3 & -S({}^A p_{c_k} - {}^A p_B) \\ 0_{3 \times 3} & 1_3 \end{bmatrix} \in \mathbb{R}^{6 \times 6} \quad (3b)$$

C. Contact Constraints

We assume that holonomic constraints of the form $c(q) = 0$ act on both the human and the robot during their interaction with the environment. The links that are in contact with the ground can be considered as end-effector links that are rigidly fixed to the ground for the duration of the contact and hence have zero velocity. Following the equation (2), this can be represented as follows for the human and the robot respectively:

$$\mathbb{J}_{c_k} \nu = 0 \quad (4a)$$

$$J_{c_k} \nu = 0 \quad (4b)$$

Differentiating the above kinematic constraints yields:

$$\begin{bmatrix} \mathbb{J}_{c_k}^b & \mathbb{J}_{c_k}^j \end{bmatrix} \begin{bmatrix} \dot{\nu}_B \\ \ddot{s} \end{bmatrix} + \begin{bmatrix} \mathbb{J}_{c_k}^b & \mathbb{J}_{c_k}^j \end{bmatrix} \begin{bmatrix} \dot{\nu}_B \\ \dot{s} \end{bmatrix} = 0 \quad (5a)$$

$$\begin{bmatrix} J_{c_k}^b & J_{c_k}^j \end{bmatrix} \begin{bmatrix} \dot{\nu}_B \\ \ddot{s} \end{bmatrix} + \begin{bmatrix} J_{c_k}^b & J_{c_k}^j \end{bmatrix} \begin{bmatrix} \dot{\nu}_B \\ \dot{s} \end{bmatrix} = 0 \quad (5b)$$

Now, during physical human-robot interaction, there is a contact between the robot and the human. We assume that these contacts can be modeled as holonomic constraints of the form $c(q, \dot{q}) = 0$. To this purpose, we consider a frame $c_m^H \in \mathcal{C}^H$ attached to the human link which is in contact with the robot. More precisely, let ${}^A T_{c_m^H}(q)$ denote the homogeneous transformation from c_m^H to the inertial frame. Similarly, we consider another frame $c_m^R \in \mathcal{C}^R$ attached to the robot link in contact with the human. Let ${}^A T_{c_m^R}(q)$ denote the

homogeneous transformation from c_m^R to the inertial frame. The relative transformation between the frames c_m^H and c_m^R is given by:

$${}^{c_m^H} T_{c_m^R} = {}^A T_{c_m^H}^{-T}(q) {}^A T_{c_m^R}(q) \quad (6)$$

When ${}^{c_m^H} T_{c_m^R}$ (or a part of it) is constant, it means that the robot and the human are in contact. By setting ${}^{c_m^H} T_{c_m^R}$ to a constant, we obtain the aforementioned holonomic constraint of the form $c(q, \dot{q}) = 0$. We assume a stable contact between the human and the robot during physical human-robot interaction, which leads to the condition that the relative velocity between the two frames c_m^H and c_m^R is zero, i.e., the two contact frames move with the same velocity with respect to the inertial frame as given by the following relation:

$${}^A v_{c_m^H} = {}^{c_m^H} X_{c_m^R} {}^A v_{c_m^R} \quad (7)$$

where ${}^{c_m^H} X_{c_m^R}$ is a frame transformation matrix. In this work we assume the contact frames to be coinciding and hence, the transformation matrix ${}^{c_m^H} X_{c_m^R} = I_{6 \times 6}$

In light of the above, the equation (7) can be written as:

$${}^A v_{c_m^H} = {}^A v_{c_m^R}, \quad (8)$$

which can be represented as follows

$$\mathbb{J}_{c_m^H} \nu = J_{c_m^R} \nu \quad (9)$$

Differentiating the equation (9) we get,

$$\begin{bmatrix} \mathbb{J}_{c_m^H}^b & \mathbb{J}_{c_m^H}^j \end{bmatrix} \begin{bmatrix} \dot{\nu}_B \\ \ddot{s} \end{bmatrix} + \begin{bmatrix} \mathbb{J}_{c_m^H}^b & \mathbb{J}_{c_m^H}^j \end{bmatrix} \begin{bmatrix} \dot{\nu}_B \\ \dot{s} \end{bmatrix} = \begin{bmatrix} \mathbb{J}_{c_m^R}^b & \mathbb{J}_{c_m^R}^j \end{bmatrix} \begin{bmatrix} \dot{\nu}_B \\ \ddot{s} \end{bmatrix} + \begin{bmatrix} \mathbb{J}_{c_m^R}^b & \mathbb{J}_{c_m^R}^j \end{bmatrix} \begin{bmatrix} \dot{\nu}_B \\ \dot{s} \end{bmatrix} \quad (10a)$$

$$\begin{bmatrix} \mathbb{J}_{c_m^H}^b & \mathbb{J}_{c_m^H}^j & -\mathbb{J}_{c_m^R}^b & -\mathbb{J}_{c_m^R}^j \end{bmatrix} \begin{bmatrix} \dot{\nu}_B \\ \ddot{s} \\ \dot{\nu}_B \\ \ddot{s} \end{bmatrix} = 0 \quad (10b)$$

Furthermore, the constraint equations (5a) (5b) (10a) and (10b) can be represented in a compact form as follows:

$$PV + Q\dot{V} = 0 \quad (11)$$

where,

$$\bullet \quad P = \begin{bmatrix} \mathbb{J}_{c_k}^b & \mathbb{J}_{c_k}^j & 0 & 0 \\ 0 & 0 & \mathbb{J}_{c_k}^b & \mathbb{J}_{c_k}^j \\ \mathbb{J}_{c_m^H}^b & \mathbb{J}_{c_m^H}^j & -\mathbb{J}_{c_m^R}^b & -\mathbb{J}_{c_m^R}^j \end{bmatrix} \in \mathbb{R}^{6 \times (n+n+12)}$$

$$\bullet \quad Q = \begin{bmatrix} \mathbb{J}_{c_k}^b & \mathbb{J}_{c_k}^j & 0 & 0 \\ 0 & 0 & \mathbb{J}_{c_k}^b & \mathbb{J}_{c_k}^j \\ \mathbb{J}_{c_m^H}^b & \mathbb{J}_{c_m^H}^j & -\mathbb{J}_{c_m^R}^b & -\mathbb{J}_{c_m^R}^j \end{bmatrix} \in \mathbb{R}^{6 \times (n+n+12)}$$

- $\mathbf{V} = \begin{bmatrix} \nu & \nu \end{bmatrix}^T \in \mathbb{R}^{n+n+2}$

D. Contact and interaction wrenches

First, observe that we can combine equation (1a) and equation (1b) to obtain a single equation of motion for the composite system as shown in Eq. (12)

$$\begin{bmatrix} \mathbb{M} & 0 \\ 0 & \mathbb{M} \end{bmatrix} \begin{bmatrix} \dot{\nu} \\ \dot{\nu} \end{bmatrix} + \begin{bmatrix} \mathbb{h} \\ \mathbb{h} \end{bmatrix} = \begin{bmatrix} \mathbb{B} & 0 \\ 0 & \mathbb{B} \end{bmatrix} \begin{bmatrix} \tau^H \\ \tau^R \end{bmatrix} + \begin{bmatrix} \mathbb{J}^T & 0 \\ 0 & \mathbb{J}^T \end{bmatrix} \begin{bmatrix} \mathbf{f}^* \\ \mathbf{f}^* \end{bmatrix} \quad (12)$$

where, $\mathbb{h} = \mathbb{C}(\mathbf{q}, \nu)\nu + \mathbb{G}(\mathbf{q})$, $\mathbf{h} = \mathbb{C}(\mathbf{q}, \nu)\nu + \mathbb{G}(\mathbf{q})$

According to the Newtonian mechanics, in the case of rigid contacts the perturbations exerted by the robot on the human is equal and opposite to the perturbation exerted by the human on the robot. As a consequence, when the external wrenches are expressed with respect to the inertial frame, the interaction wrenches \mathbf{f} can be written as follows:

$$\mathbf{f} = \mathbf{f}_m = -\mathbf{f}_m \quad (13)$$

As a consequence, the equation (12) can be written in a compact form as follows:

$$\mathbf{M}\dot{\mathbf{V}} + \mathbf{h} = \mathbf{B}\boldsymbol{\tau} + \mathbf{J}^T \mathbf{f}^* \quad (14)$$

where $\mathbf{f}^* = [f \quad \mathbb{f}_e \quad f_e]^T \in \mathbb{R}^{6(n_m+n_e+n_e)}$ and \mathbf{J} a proper jacobian matrix. This equation implies that

$$\dot{\mathbf{V}} = \mathbf{M}^{-1}[\mathbf{B}\boldsymbol{\tau} + \mathbf{J}^T \mathbf{f}^* - \mathbf{h}] \quad (15)$$

We make use of the equation (15) in the constraint equation (11)

$$\begin{aligned} \mathbf{P}\mathbf{V} + \mathbf{Q}\mathbf{M}^{-1}[\mathbf{B}\boldsymbol{\tau} + \mathbf{J}^T \mathbf{f}^* - \mathbf{h}] &= 0 \\ \Rightarrow \mathbf{Q}\mathbf{M}^{-1}\mathbf{J}^T \mathbf{f}^* &= -[\mathbf{Q}\mathbf{M}^{-1}[\mathbf{B}\boldsymbol{\tau} - \mathbf{h}] + \mathbf{P}\mathbf{V}] \\ \Rightarrow \mathbf{f}^* &= -\Gamma^{-1}[\mathbf{Q}\mathbf{M}^{-1}[\mathbf{B}\boldsymbol{\tau} - \mathbf{h}] + \mathbf{P}\mathbf{V}] \end{aligned}$$

where, $\Gamma = \mathbf{Q}\mathbf{M}^{-1}\mathbf{J}^T$

Furthermore,

$$\mathbf{f}^* = -\Gamma^{-1}\mathbf{Q}\mathbf{M}^{-1}\mathbf{B}\boldsymbol{\tau} + \Gamma^{-1}\mathbf{Q}\mathbf{M}^{-1}\mathbf{h} - \Gamma^{-1}\mathbf{P}\mathbf{V} \quad (17)$$

Through coupled-dynamics, equation (17) shows that the external wrenches are a function of system configuration \mathbf{q} , $\dot{\mathbf{q}}$, system velocity ν , $\dot{\nu}$, and joint torques τ^H , τ^R . This can be represented as a function $\mathbf{f}^* = g(\mathbf{q}, \dot{\mathbf{q}}, \nu, \dot{\nu}, \tau^H, \tau^R)$. This relation can be further decomposed as,

$$\mathbf{f}^* = \mathbf{G}_1\tau^H + \mathbf{G}_2\tau^R + \mathbf{G}_3(\mathbf{q}, \dot{\mathbf{q}}, \nu, \dot{\nu}) \quad (18)$$

where,

- $\mathbf{G}_1 \in \mathbb{R}^{6(n_m+n_e+n_e) \times n}$
- $\mathbf{G}_2 \in \mathbb{R}^{6(n_m+n_e+n_e) \times n}$
- $\mathbf{G}_3 \in \mathbb{R}^{6(n_m+n_e+n_e)}$

III. PARTNER-AWARE CONTROL

Let $\chi \in \mathbb{R}^p$ be a robot-related quantity of dimension p that is assumed to have a linear map to the robot's velocity, i.e.:

$$\chi = \mathbf{J}_\chi(\mathbf{q}) \nu \quad (19)$$

where $\mathbf{J}_\chi(\mathbf{q}) \in \mathbb{R}^{p \times (n+6)}$. Let χ_d denote the desired value of χ , and $\tilde{\chi} = \chi - \chi_d$ the error to be minimized. On time differentiating (19) and by substituting the robot acceleration $\dot{\nu}$ with its expression obtained from the model (1b) one can observe that the acceleration $\dot{\chi}$ depends upon the robot torques τ^R , namely, $\dot{\chi} = \dot{\chi}(\tau^R)$. Then, a classical approach for the control of the robot quantity χ_d consists of finding the robot joint torques τ^R such that

$$\dot{\chi} = \dot{\chi}_d - k_d \tilde{\chi} - k_p \int_0^t \tilde{\chi} ds, \quad k_d, k_p > 0 \quad (20)$$

This is a classical feedback linearisation approach [37]. In the language of optimisation theory, the above feedback linearisation control task can be framed in the following optimisation problem

$$\tau^R = \arg \min_{\tau^R} |\dot{\chi}(\tau^R) - \dot{\chi}_d + k_d \tilde{\chi} + k_p \int_0^t \tilde{\chi} ds|^2 \quad (21a)$$

s.t.

$$\mathbf{M}\dot{\mathbf{V}} + \mathbf{h} = \mathbf{B}\boldsymbol{\tau} + \mathbf{J}^T \mathbf{f}^* \quad (21b)$$

$$\mathbf{P}\mathbf{V} + \mathbf{Q}\dot{\mathbf{V}} = 0 \quad (21c)$$

A. Task based partner-aware robot control

Although the feedback linearisation approach is robust, it fundamentally is agnostic to any interaction from an external agent. This is evident from Eq. (20), since no human quantity appears on the right hand side of this equation. Alternatively, instead of completely canceling out any external interaction by the feedback control action, it is desirable to *exploit* it to accomplish the robot's task. This poses, however, the question of quantifying the human help with respect to the robot task. In our previous approach [38] we relied on using the interaction wrench estimates from the robot as human intent information. This introduces an algebraic loop in the control design as the wrench estimates from the robot are computed using the robot joint torques [39]. Instead, a sound approach is to leverage the joint torques of the agent interacting with the robot. Additionally, in the case of humans interacting with the robot, considering the joint torques opens new possibilities to investigate and optimize human ergonomics.

The following lemma proposes control laws that exploit the human contribution towards the achievement of the robot control objective, thus actively taking into account the physical human-robot interaction. The associated analysis is based on considering the *energy* of the robot control task.

Lemma 1: Assume that the control objective is to asymptotically stabilize the following point

$$\left(\tilde{\chi}, \int \tilde{\chi} ds \right) = (0, 0) \quad (22)$$

Apply the following robot torques to the robot system (1b)

$$\tau^R = -\Delta^\dagger [\Lambda + K_D \tilde{\chi} + \max(0, \alpha) \tilde{\chi}^\parallel] + N \Delta \tau_0^R \quad (23)$$

with

- $\Delta = K_d \mathbf{J}_\chi \mathbf{M}^{-1} [\mathbf{B} + \mathbf{J}^T \mathbf{G}_2] \in \mathbb{R}^{p \times n}$

- N_{Δ} the null-space projector of the matrix Δ ;
- τ_0^R a free n -dimensional vector;
- $\Delta = K_d [[J_{\chi} M^{-1} J^T] \bar{G}_3(q, q, \nu, \nu) - J_{\chi} M^{-1} h + J_{\chi} \nu + K_p \int_0^t (\chi - \chi_d) ds - \dot{\chi}_d] \in \mathbb{R}^p$
- $K_D \in \mathbb{R}^{p \times p}$ is a symmetric, positive-definite matrix
- $\alpha \in \mathbb{R}$ is a component proportional to the human joint torques τ^H projected along $\tilde{\chi}^{\parallel}$ i.e., the direction parallel to $\tilde{\chi}$

Assume that the matrix Δ is full rank matrix $\forall t \in \mathbb{R}^+$. Then

- The trajectories $(\tilde{\chi}, \int \tilde{\chi} ds)$ are globally bounded
- The equilibrium point (22) is stable

A sketch of the proof of *Lemma 1* is outlined in the appendix. Observe that the control law (23) includes a degree of redundancy under the assumption that the matrix Δ is fat, i.e. the dimension of the robot control task is lower than the robot actuation. As a consequence, the free vector τ_0^R can be used for other control purposes like robot postural task.

IV. EXPERIMENTS

In case of complex humanoids robots, state-of-the-art whole-body controllers often consider controlling the robot momentum [40] [13] and accordingly the Eq. (19) becomes,

$$L = J_{cmm}(q) \nu \quad (24)$$

where, J_{cmm} is the centroidal momentum matrix.

The primary control objective of the robot is momentum control while performing the stand-up from a chair task. The robot will make use of any assistance provided by the interacting agent to achieve this task. There are four states designed in the controller. Fig. 2 highlights the four states of the robot in simulation. The robotic platform used in our experiments is iCub humanoid robot [41]. During the state 1, the robot balances on a chair and state 2 is reached by moving the robot's center of mass (CoM) forward. The robot reaches state 3 by lifting the center of mass from the seated chair and then finally reaches state 4 by standing-up fully erect. The blue circles indicate the contact locations between the robot and the environment. Accordingly, the *legs* of the robot are in contact with the chair during the states 1 and 2 while the *feet* of the robot are in contact with the ground during the states 3,4. The green lines indicate the normal forces at each of the contact locations.

Originally for the human side of the experiment we intended to use a human subject in a sensorized suit providing real-time estimation of human dynamics [38]. However, at the time of our experiments the system was unavailable and this motivated us to get creative to make use of two iCub robots together with one acting as an external interacting agent. The experimental scenario is as shown in the Fig. 3 where the *green* iCub robot is acting as an interacting agent and it will physically interact with the *purple* robot through a metallic pipe of negligible dynamics. The hands of the iCub

robot are quite fragile and are not designed to make sustained power grasps. This posed quite a challenge during our experiments. Mechanical coupling of the hands to the bar using just the fingers is hard to maintain during the entire duration of the experiment because of the hardware limitations of the fingers motors. So, we took additional precautions of using tape to ensure strong coupling throughout the experiment.

The robot acting as an interacting agent is position controlled. A predetermined trajectory generated using a minimum-jerk trajectory generator [42] is given as a reference to the torso pitch, shoulder pitch and elbow joints of the robot. This motion imitates a pulling up motion as a human would perform. The joint motion is indicated in Fig. 4a and the associated joint torques are shown in Fig. 4b.

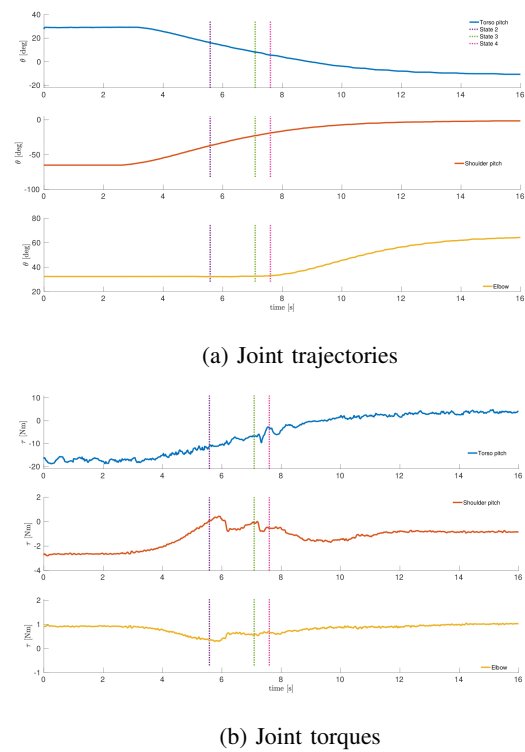


Fig. 4: Interacting agent joint quantities

V. RESULTS

The controller takes center of mass trajectory reference to make the *purple* iCub robot perform the stand-up motion. The time evolution of center of mass tracking is shown in Fig. 5. The vertical lines indicate the instances at which the state transitions occur. The overall center of mass tracking is good except in between the states 3 and 4. It is because at the beginning of state 3 the robot switches contacts from legs seated on chair to its feet. This contact switching creates a momentary sway in center of mass tracking but eventually the robot recovers from it.

The time evolution of the linear and angular momentum of the robot are shown in Fig. 6. The overall robot momentum is maintained close to zero except starting from state 3. Understandably this results from the impact at the contact

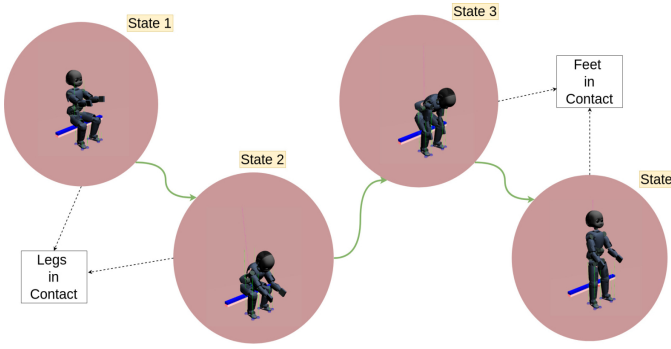


Fig. 2: State machine of the controller



Fig. 3: Experimental scenario with two iCub robots involved in physical interaction (picture is only representative)

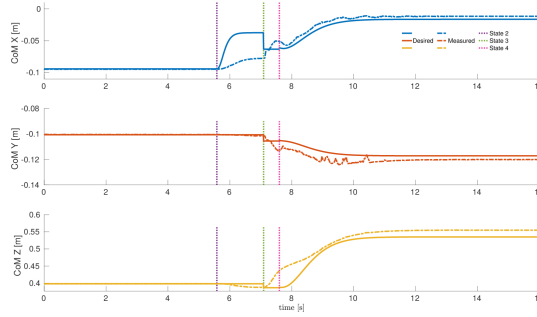


Fig. 5: Time evolution of the desired and measured CoM trajectory while performing stand-up motion on application of the control law (23)

switching as explained previously. However, the momentum error converges to zero eventually and the robot becomes stable.

VI. CONCLUSIONS AND FUTURE WORK

The classical approach of feedback linearisation helps in building robust controllers for robotic systems but ignores any helpful interaction made by an external agent. In this paper, we presented a coupled-dynamics approach to build partner-aware controllers that exploits useful interaction for successful task completion. Further, we demonstrated the abilities of our controller by performing physical interaction experiments with two complex humanoid robots. In the near future, we plan to conduct physical human-robot interaction experiments and present the results with full proof of stability and convergence of our control law.

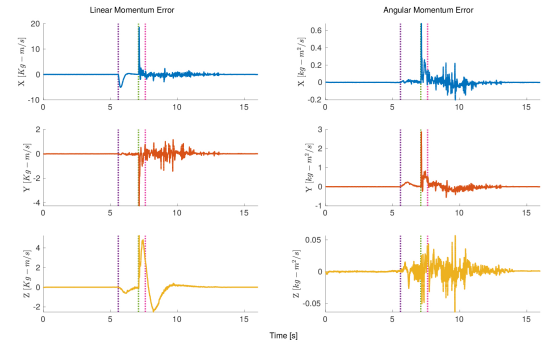


Fig. 6: Time evolution of the linear and angular momentum while performing stand-up motion on application of the control law (23)

APPENDIX: SKETCH OF PROOF OF LEMMA 1

Proof: The stability of $\tilde{\chi}$ can be analyzed by considering the following Lyapunov function:

$$V = \frac{K_d}{2} \|\chi - \chi_d\|^2 + \frac{K_p}{2} \left\| \int_0^t (\chi - \chi_d) ds \right\|^2 \quad (25)$$

where $K_d, K_p \in \mathbb{R}^{p \times p}$ are two symmetric, positive-definite matrices. Now, on differentiating (25) and using the robot dynamics (1b) along with the force decomposition (18) obtained through coupled-dynamics, we get:

$$\dot{V} = -\tilde{\chi}^T K_D \tilde{\chi} - \max(0, \alpha) \|\tilde{\chi}\|^2 \quad (26)$$

The fact that the human joint torques help the robot to perform a control action is encompassed in the right hand side of above equation: a positive α makes the Lyapunov function decrease faster. Thus the control law (23) ensures that $\dot{V} \leq 0$ which proves that the trajectories are globally bounded. From lyapunov theory, as $\dot{V} \leq 0$ in the neighborhood of the point $(0, 0)$ the equilibrium point (22) is stable. The complete proof of *Lemma 1* is beyond the scope of this paper due to the space limitations and it will be presented in full in our forthcoming journal publication.

ACKNOWLEDGMENT

The authors would like to thank Yue Hu, Stefano Dafarra, Giulio Romualdi and, Aiko Dinali for their support in conducting experiments.

REFERENCES

[1] D. P. Losey, C. G. McDonald, E. Battaglia, and M. K. O’Malley, “A review of intent detection, arbitration, and communication aspects of shared control for physical human–robot interaction,” *Applied Mechanics Reviews*, vol. 70, no. 1, p. 010804, 2018.

[2] M. A. Goodrich, A. C. Schultz *et al.*, “Human–robot interaction: a survey,” *Foundations and Trends® in Human–Computer Interaction*, vol. 1, no. 3, pp. 203–275, 2008.

[3] S. Caux, E. Mateo, and R. Zapata, “Balance of biped robots: special double-inverted pendulum,” in *Systems, Man, and Cybernetics, 1998. 1998 IEEE International Conference on*, vol. 4. IEEE, 1998, pp. 3691–3696.

[4] K. Hirai, M. Hirose, Y. Haikawa, and T. Takenaka, “The development of honda humanoid robot,” in *Robotics and Automation, 1998. Proceedings. 1998 IEEE International Conference on*, vol. 2. IEEE, 1998, pp. 1321–1326.

[5] S.-H. Hyon, J. G. Hale, G. Cheng *et al.*, “Full-body compliant human–humanoid interaction: Balancing in the presence of unknown external forces,” *IEEE Trans. Robotics*, vol. 23, no. 5, pp. 884–898, 2007.

[6] B. J. Stephens and C. G. Atkeson, “Dynamic balance force control for compliant humanoid robots,” in *Intelligent Robots and Systems (IROS), 2010 IEEE/RSJ International Conference on*. IEEE, 2010, pp. 1248–1255.

[7] A. Herzog, L. Righetti, F. Grimminger, P. Pastor, and S. Schaal, “Balancing experiments on a torque-controlled humanoid with hierarchical inverse dynamics,” in *Intelligent Robots and Systems (IROS 2014), 2014 IEEE/RSJ International Conference on*. IEEE, 2014, pp. 981–988.

[8] T. Koolen, S. Bertrand, G. Thomas, T. De Boer, T. Wu, J. Smith, J. Englsberger, and J. Pratt, “Design of a momentum-based control framework and application to the humanoid robot atlas,” *International Journal of Humanoid Robotics*, vol. 13, no. 01, p. 1650007, 2016.

[9] A. Hofmann, M. Popovic, and H. Herr, “Exploiting angular momentum to enhance bipedal center-of-mass control,” in *Robotics and Automation, 2009. ICRA’09. IEEE International Conference on*. IEEE, 2009, pp. 4423–4429.

[10] F. Nori, S. Traversaro, J. Eljaik, F. Romano, A. Del Prete, and D. Pucci, “icub whole-body control through force regulation on rigid non-coplanar contacts,” *Frontiers in Robotics and AI*, vol. 2, p. 6, 2015.

[11] C. Ott, M. A. Roa, and G. Hirzinger, “Posture and balance control for biped robots based on contact force optimization,” in *Humanoid Robots (Humanoids), 2011 11th IEEE-RAS International Conference on*. IEEE, 2011, pp. 26–33.

[12] P. M. Wensing and D. E. Orin, “Generation of dynamic humanoid behaviors through task-space control with conic optimization,” in *Robotics and Automation (ICRA), 2013 IEEE International Conference on*. IEEE, 2013, pp. 3103–3109.

[13] G. Nava, F. Romano, F. Nori, and D. Pucci, “Stability analysis and design of momentum-based controllers for humanoid robots,” in *Intelligent Robots and Systems (IROS), 2016 IEEE/RSJ International Conference on*. IEEE, 2016, pp. 680–687.

[14] E. A. Mattar, H. J. Al-Junaid, and H. H. Al-Seddiqi, “Biomimetic based eeg learning for robotics complex grasping and dexterous manipulation,” in *Biomimetic Prosthetics*. InTech, 2018.

[15] M. Sarac, E. Koyas, A. Erdogan, M. Cetin, and V. Patoglu, “Brain computer interface based robotic rehabilitation with online modification of task speed,” in *Rehabilitation Robotics (ICORR), 2013 IEEE International Conference on*. IEEE, 2013, pp. 1–7.

[16] D. P. McMullen, G. Hotson, K. D. Katyal, B. A. Wester, M. S. Fifer, T. G. McGee, A. Harris, M. S. Johannes, R. J. Vogelstein, A. D. Ravitz *et al.*, “Demonstration of a semi-autonomous hybrid brain–machine interface using human intracranial eeg, eye tracking, and computer vision to control a robotic upper limb prosthetic,” *IEEE Transactions on Neural Systems and Rehabilitation Engineering*, vol. 22, no. 4, pp. 784–796, 2014.

[17] A. Radmand, E. Scheme, and K. Englehart, “A characterization of the effect of limb position on emg features to guide the development of effective prosthetic control schemes,” in *Engineering in Medicine and Biology Society (EMBC), 2014 36th Annual International Conference of the IEEE*. IEEE, 2014, pp. 662–667.

[18] S. Au, M. Berniker, and H. Herr, “Powered ankle-foot prosthesis to assist level-ground and stair-descent gaits,” *Neural Networks*, vol. 21, no. 4, pp. 654–666, 2008.

[19] R. Song, K.-y. Tong, X. Hu, L. Li *et al.*, “Assistive control system using continuous myoelectric signal in robot-aided arm training for patients after stroke,” *IEEE transactions on neural systems and rehabilitation engineering*, vol. 16, no. 4, pp. 371–379, 2008.

[20] Y. Zhou, Y. Fang, J. Zeng, K. Li, and H. Liu, “A multi-channel emg-driven fes solution for stroke rehabilitation,” in *International Conference on Intelligent Robotics and Applications*. Springer, 2018, pp. 235–243.

[21] E. Cho, R. Chen, L.-K. Merhi, Z. Xiao, B. Pousett, and C. Menon, “Force myography to control robotic upper extremity prostheses: a feasibility study,” *Frontiers in bioengineering and biotechnology*, vol. 4, p. 18, 2016.

[22] H. K. Yap, A. Mao, J. C. Goh, and C.-H. Yeow, “Design of a wearable fmg sensing system for user intent detection during hand rehabilitation with a soft robotic glove,” in *Biomedical Robotics and Biomechatronics (BioRob), 2016 6th IEEE International Conference on*. IEEE, 2016, pp. 781–786.

[23] M. Rasouli, K. Cheellamuthu, J.-J. Cabibihan, and S. L. Kukreja, “Towards enhanced control of upper prosthetic limbs: A force-myographic approach,” in *Biomedical Robotics and Biomechatronics (BioRob), 2016 6th IEEE International Conference on*. IEEE, 2016, pp. 232–236.

[24] L. Peternel, N. Tsagarakis, D. Caldwell, and A. Ajoudani, “Robot adaptation to human physical fatigue in human–robot co-manipulation,” *Autonomous Robots*, pp. 1–11, 2018.

[25] A. Bussy, A. Kheddar, A. Crosnier, and F. Keith, “Human–humanoid haptic joint object transportation case study,” in *Intelligent Robots and Systems (IROS), 2012 IEEE/RSJ International Conference on*. IEEE, 2012, pp. 3633–3638.

[26] A. Bussy, P. Gergondet, A. Kheddar, F. Keith, and A. Crosnier, “Proactive behavior of a humanoid robot in a haptic transportation task with a human partner,” in *RO-MAN, 2012 IEEE*. IEEE, 2012, pp. 962–967.

[27] S. Ikemoto, H. B. Amor, T. Minato, B. Jung, and H. Ishiguro, “Physical human–robot interaction: Mutual learning and adaptation,” *IEEE robotics & automation magazine*, vol. 19, no. 4, pp. 24–35, 2012.

[28] L. Peternel and J. Babić, “Learning of compliant human–robot interaction using full-body haptic interface,” *Advanced Robotics*, vol. 27, no. 13, pp. 1003–1012, 2013.

[29] P. Donner and M. Buss, “Cooperative swinging of complex pendulum-like objects: Experimental evaluation,” *IEEE Transactions on Robotics*, vol. 32, no. 3, pp. 744–753, 2016.

[30] B. Reily, F. Han, L. E. Parker, and H. Zhang, “Skeleton-based bio-inspired human activity prediction for real-time human–robot interaction,” *Autonomous Robots*, vol. 42, no. 6, pp. 1281–1298, 2018.

[31] E. Kyrkjebø, “Inertial human motion estimation for physical human–robot interaction using an interaction velocity update to reduce drift,” in *Companion of the 2018 ACM/IEEE International Conference on Human–Robot Interaction*. ACM, 2018, pp. 163–164.

[32] S. S. Rautaray and A. Agrawal, “Vision based hand gesture recognition for human computer interaction: a survey,” *Artificial Intelligence Review*, vol. 43, no. 1, pp. 1–54, 2015.

[33] D. J. Agrawante, A. Cherubini, A. Bussy, P. Gergondet, and A. Kheddar, “Collaborative human–humanoid carrying using vision and haptic sensing,” in *Robotics and Automation (ICRA), 2014 IEEE International Conference on*. IEEE, 2014, pp. 607–612.

[34] A. De Santis, V. Lippiello, B. Siciliano, and L. Villani, “Human–robot interaction control using force and vision,” in *Advances in Control Theory and Applications*. Springer, 2007, pp. 51–70.

[35] J. E. Marsden and T. S. Ratiu, *Introduction to Mechanics and Symmetry: A Basic Exposition of Classical Mechanical Systems*. Springer Publishing Company, Incorporated, 2010.

[36] R. Featherstone, *Rigid Body Dynamics Algorithms*. Secaucus, NJ, USA: Springer-Verlag New York, Inc., 2007.

[37] W. Khalil and E. Dombre, *Modeling, identification and control of robots*. Butterworth-Heinemann, 2004.

[38] F. Romano, G. Nava, M. Azad, J. amernik, S. Dafarra, O. Dermy, C. Latella, M. Lazzaroni, R. Lober, M. Lorenzini, D. Pucci, O. Sigaud, S. Traversaro, J. Babić, S. Ivaldi, M. Mistry, V. Padois, and F. Nori, “The codyco project achievements and beyond: Toward human aware whole-body controllers for physical human robot interaction,” *IEEE Robotics and Automation Letters*, vol. 3, no. 1, pp. 516–523, Jan 2018.

[39] F. Nori, S. Traversaro, J. Eljaik, F. Romano, A. Del Prete, and D. Pucci, “icub whole-body control through force regulation on rigid

noncoplanar contacts,” *Frontiers in Robotics and AI*, vol. 2, no. 6, 2015.

[40] D. Pucci, F. Romano, S. Traversaro, and F. Nori, “Highly dynamic balancing via force control,” in *2016 IEEE-RAS 16th International Conference on Humanoid Robots (Humanoids)*, Nov 2016, pp. 141–141.

[41] G. Metta, L. Natale, F. Nori, G. Sandini, D. Vernon, L. Fadiga, C. Von Hofsten, K. Rosander, M. Lopes, J. Santos-Victor *et al.*, “The icub humanoid robot: An open-systems platform for research in cognitive development,” *Neural Networks*, vol. 23, no. 8-9, pp. 1125–1134, 2010.

[42] U. Pattacini, F. Nori, L. Natale, G. Metta, and G. Sandini, “An experimental evaluation of a novel minimum-jerk cartesian controller for humanoid robots,” in *2010 IEEE/RSJ International Conference on Intelligent Robots and Systems*, Oct 2010, pp. 1668–1674.